ISSN 2347 - 3983
Volume 1, No.2, October 2013
International Journal of Emerging Trends in Engineering Research
Available Online at http://warse.org/pdfs/2013/ijeter01122013.pdf

Incorporation of different FACTS devices in Transmission system for minimization of losses

A.Vamsi Kumar Reddy[1], Dr.N.Visali[2]
[1]jntuacep, pg scholar india, avkreee@gmail.com
[2]jntuacep,professor,india, nvisali@gmail.com

ABSTRACT

This paper presents an AC Transmission system power flow controlled by injecting a compensating voltage in series with the line and injecting reactive power in shunt with the bus. Static Synchronous Series Compensator (SSSC) and Static Synchronous Compensator (STATCOM) are utilized as a series and shunt compensation, respectively while Unified Power Flow Controller (UPFC) is considered as a shunt-series compensator.The prediction of dynamic voltage collapse at the buses is found by calculating voltage collapse prediction index (VCPI) for placement of shunt FACTS devices and Fast voltage stability index (FVSI) for placement of series FACTS devices. This paper covers, in depth, the modeling and simulation methods required for a thorough study of the steady-state operation of electrical power systems with these flexible AC Transmission Systems (FACTS) controllers. A thorough grounding on the theory and practice of positive sequence power flow is offered here. MATLAB® codes are utilized for the implementation of the three devices in the Newton-Raphson algorithm. Power flow control ranges are evaluated for standard 14-bus system. Results are reported and studies are presented to illustrate and compare the effectiveness of the STATCOM, SSSC and UPFC.

Keywords: FACTS, flexible AC transmission systems, MATLAB, Newton-Raphson algorithm, power flow, Static Synchronous Compensator, STATCOM, Static Synchronous Series Compensator, SSSC, Unified Power Flow Controller, UPFC),Voltage collapse precedence index ,VCPI,fast voltage stability index, FVSI.

1. INTRODUCTION

With regards to the deregulation of the power system industry and higher industrial demands, transmission facilities are being excessively used. This provides the need for building new transmission lines and electricity generating plants, a solution that is costly to implement and that involves long construction times and opposition from pressure groups. So other ways of maximizing the power transfers of existing transmission facilities while simultaneously maintaining acceptable levels of network reliability and stability should be considered.

Recent advancements in power electronics have proven to satisfy this need by introducing the concept of flexible AC transmission system (FACTS). FACTS-devices can be utilized to increase the transmission capacity, improve the stability and dynamic behavior or ensure better power quality in modern power systems. Their main capabilities are reactive power compensation, voltage control, and power flow control [4]. Due to their controllable power electronics, FACTS-devices always provide fast control actions in comparison to conventional devices like switched compensation or phase shifting transformers with mechanical on-load tap changers.
The first generation of FACTS-devices was mechanically controlled capacitors and inductors. The second generation of FACTS devices replaced the mechanical switches by the thyristor valve control. The second generation gave a noticeable improvement in the speed and the enhancement in concept to mitigate the disturbances. The third generation uses the concept of voltage source converter based devices. These devices provide multi-dimensional control of the power system parameters [7], [8].

The voltage collapse prediction index provides better prediction of dynamic voltage collapse. Which is proposed by glamorization [11].In this paper analysis of voltage behavior has been approached using static techniques, which have been widely used on voltage stability analysis. These indices provide reliable information about proximity of voltage instability in a power system usually, their values changes between 0 (no load) and 1 (voltage collapse).For a typical transmission line, the line stability index (FVSI) is calculated. It is well known that power flow calculations are the most frequently performed routine power network calculations, which can be used in power system planning, operational planning, and operation/control. It is also considered as the fundamental of power system network calculations. The calculations are required for the analysis of steady-state as well as dynamic performance of power systems. Among the power flow methods proposed, the Newton's method technique [2] has

been considered as the power flow solution technique for large-scale power system analysis. A detailed review of power flow methods can be found in [4]. This paper deals with the steady state models of STATCOM [1], [4] SSSC [9], [10], and UPFC [1], [4], [8] which can be combined in Newton-Raphson load flow algorithm.

2. POWER FLOW CONTROL

The power transmission line can be represented by a two-bus system "k" and "m" in ordinary form [6]. The active power transmitted between bus nodes k and m is given by:

$$P = \frac{V_k * V_m}{X}\sin(\delta_k - \delta_m) \quad (1)$$

Where $\boldsymbol{\delta_k}$ and $\boldsymbol{\delta_m}$ are the voltages at the nodes, $(\boldsymbol{\delta_k} - \boldsymbol{\delta m})$ the angle between the voltages and, the line impedance. The power flow can be controlled by altering the voltages at a node, the impedance between the nodes and the angle between the end voltages. The reactive power is given by:

$$Q = \frac{V_k^2}{X} - \frac{V_m * V_k}{X}\cos(\boldsymbol{\delta_k} - \boldsymbol{\delta m}) \quad (2)$$

2.1 Newton-raphson power flow

In large-scale power flow studies, the Newton-Raphson [8] has proved most successful owing to its strong convergence characteristics. The power flow Newton-Raphson algorithm is expressed by the following relationship:

$$\begin{bmatrix}\Delta P \\ \Delta Q\end{bmatrix} = \begin{bmatrix}\frac{\partial P}{\partial \theta} & V\frac{\partial P}{\partial V} \\ \frac{\partial Q}{\partial \theta} & V\frac{\partial Q}{\partial V}\end{bmatrix}\begin{bmatrix}\Delta\theta \\ \frac{\Delta V}{V}\end{bmatrix} \quad (3)$$

Where **ΔP** and **ΔQ** are bus active and reactive power mismatches, while **θ** and **V** are bus magnitude and angle, respectively.

3.VOLTAGE COLLAPSE PREDICTION INDEX:

Voltage stability index is proposed based on the voltage phasor info of the taking part buses within the system and also the network admittance matrix. using the measured voltage phasor and also the network admittance matrix of the system, the voltage collapse prediction index (VCPI) is calculated at each bus. the value of the index determines the proximity to voltage collapse at a bus. The technique comes from the fundamental power flow equation, that is applicable for any variety of buses in an exceedingly system. the power flow equations are resolved by Newton Raphson methodology, that creates a partial matrix. By setting the determinant of the matrix to zero, the index at bus k is written as follows:

$$\mathrm{VCPI_k} = \left|1 - \frac{\sum_{m=1,m\neq k}^{N} V'_m}{V_k}\right| \quad (4)$$

Where,

$$V'_m = \frac{Y_{km}}{\sum_{j=1,j\neq k}^{N} Y_{kj}} V_m$$

Vk is the voltage phasor at bus k
Vm is the voltage phasor at bus m
Ykm is the admittance between bus k and m
Ykj is the admittance between bus k and j
k is the monitoring bus
m is the other bus connected to bus k
N is the bus set of the system

The value of VCPI varies between zero and one. If the index is zero, the voltage at bus k is taken into account stable and if the index is unity, a voltage collapse is claimed to occur. VCPI is calculated solely with info of voltage phasor of taking part buses and impedance of relating lines. The calculation is straightforward while not matrix conversion. The technique offers quick calculation which may be applied for on-line watching of the power system

4. MODELING OF POWER SYSTEMS WITH STATCOM

It is acceptable to expect that for the aim of positive sequence power flow analysis the STATCOM will be represented by a synchronous voltage source with maximum and minimum voltage magnitude limits [4]. The synchronous voltage source stands for the fundamental Fourier series component of the switched voltage waveform at the AC converter terminal of the STATCOM. The bus at which the STATCOM is connected is represented as a PV bus, which may change to a PQ bus in the case of limits being violated. In this case, the generated or absorbed reactive power would reach to the maximum limit. The STATCOM equivalent circuit shown in Figure 1 is used to obtain the mathematical model of the controller for incorporation in power flow algorithms [2].

The power flow equations for the STATCOM are derived below:

$$E_{vR} = V_{vR}(\cos\delta_{vR} + J\sin\delta_{vR}) \quad (5)$$

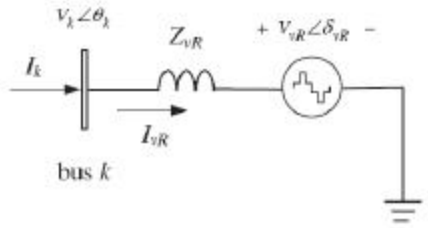

Figure 1: STATCOM Equivalent Circuit

Based on the shunt connection shown in Figure 1, the following may be written:

$$S_{vR} = V_{vR}I_{vR}^{*} = V_{vR}Y_{vR}^{*}(V_{vR}^{*}) - V_k^{*} \qquad (6)$$

After performing some complex operations, the following active and reactive power equations are obtained for the converter and bus k, respectively:

$$P_{vR} = -V_{vR}^2 G_{vR} + V_{vR}V_k[G_{vR}\cos(\delta_{vR} - \theta_k) + B_{vR}\sin(\delta_{vR} - \theta_k)] \qquad (7)$$

$$Q_{vR} = -V_{vR}^2 B_{vR} + V_{vR}V_k[G_{vR}\sin(\delta_{vR} - \theta_k) - B_{vR}\cos(\delta_{vR} - \theta_k)] \qquad (8)$$

$$P_k = V_k^2 G_{vR} + V_k V_{vR}[G_{vR}\cos(\theta_k - \delta_{vR}) + B_{vR}\sin(\theta_k - \delta_{vR})] \qquad (9)$$

$$Q_k = -V_k^2 B_{vR} + V_{vR}V_k[G_{vR}\sin(\theta_k - \delta_{vR}) - B_{vR}\cos(\theta_k - \delta_{vR})] \qquad (10)$$

Using these power equations, the linearized STATCOM model is given below, where the voltage magnitude V_{vR} and phase angle δ_{vR} are taken to be the state variables [4]

$$\begin{bmatrix} \Delta P_k \\ \Delta Q_k \\ \Delta P_{vR} \\ \Delta P_{vR} \end{bmatrix} = \begin{bmatrix} \frac{\partial P_k}{\partial \theta_k} & \frac{\partial P_k}{\partial V_k}V_k & \frac{\partial P_k}{\partial \delta_{vR}} & \frac{\partial P_k}{\partial V_{vR}}V_{vR} \\ \frac{\partial Q_k}{\partial \theta_k} & \frac{\partial Q_k}{\partial V_k}V_k & \frac{\partial Q_k}{\partial \delta_{vR}} & \frac{\partial Q_k}{\partial V_{vR}}V_{vR} \\ \frac{\partial P_{vR}}{\partial \theta_k} & \frac{\partial P_{vR}}{\partial V_k}V_k & \frac{\partial P_{vR}}{\partial \delta_{vR}} & \frac{\partial P_{vR}}{\partial V_{vR}}V_{vR} \\ \frac{\partial Q_{vR}}{\partial \theta_k} & \frac{\partial Q_{vR}}{\partial V_k}V_k & \frac{\partial Q_{vR}}{\partial \delta_{vR}} & \frac{\partial Q_{vR}}{\partial V_{vR}}V_{vR} \end{bmatrix} \begin{bmatrix} \Delta\theta_k \\ \frac{\Delta V_k}{V_K} \\ \Delta\delta_{vR} \\ \frac{\Delta V_{vR}}{V_{vR}} \end{bmatrix} \qquad (11)$$

5. FAST VOLTAGE STABILITY INDEX (FVSI)

Fast voltage stability index (FVSI) is formulated this as the measuring instrument in predicting thevoltage stability condition in the system.Taking the symbols 'i' as the sending bus and 'j' as the receiving bus. Hence, the fast voltage stability index,FVSI can be defined by:

$$FVSI_{ij} = \frac{4Z_{ij}^2\, Q_j}{V_i^2 X_{ij}} \qquad (12)$$

Where: $\mathbf{Z_{ij}}$= line impedance
X_{ij}= line reactance
Qj = reactive power at the receiving end
Vi = sending end voltage
The value of FVSI that is evaluated close to 1.00 indicates that the particular line is closed to its instability pointwhich may lead to voltage collapse in the entire system. To maintain a secure condition the value of FVSl should be maintained well less than 1.00.

6. MODELING OF POWER SYSTEMS WITH SSSC

Figure 2 shows the circuit model of an SSSC connected to link k–m.The objective for the addition of SSSC is to control the active power $P_k$to a target value [10].The SSSC is modeled as a voltage source (V_{vR}) with adjustable magnitude and angle in series with an impedance.
The real part of this impedance represents the ohmic losses of the power electronic devices and the coupling transformer. The imaginary part of this impedance represents the leakage reactance of the coupling transformer. The admittance $Y_s$shown in Figure 2 represents the combined admittances of the SSSC and the line to which it is connected [9]. The presence of V_{cR}introduces two new variables (V_{cR} *and* δ_{cR}) to the power flow problem. Thus, two new equations are needed for power flow solution. One of these equations is found by equating $P_k$to its target value, and the other one is found using the fact that the power consumed by the source V_{cR} is equal to zero. The power flow equations for all buses of the power system with SSSC in place are the same as those of the system without SSSC, except for Buses k and m [8].

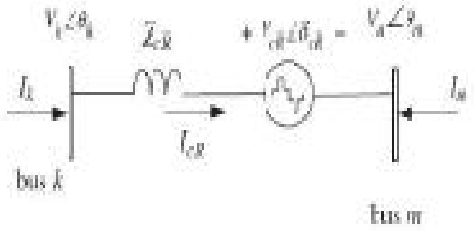

Figure 2: SSSC Equivalent Circuit

The SSSC voltage source is:

$$E_{cR} = V_{cR}(\cos\delta_{cR} + J\sin\delta_{cR}) \quad (13)$$

The magnitude V_{cR} and phase angle δ_{cR} of the voltage source representing the series converter are controlled between limits $(V_{cRmin} \le V_{cR} \le V_{cRmax})$ and $(0 \le \delta_{cR} \le 2\pi)$ respectively. Based on the equivalent circuit shown in Figure 2 and Equations (11), the active and reactive power equations at bus k are:

$$P_k = V_k^2 G_{kk} + V_k V_m [G_{km}\cos(\theta_k - \theta_m) + B_{km}\sin(\theta_k - \theta_m)] + V_k V_{cR}[G_{km}\cos(\theta_k - \delta_{cR}) + B_{km}\sin(\theta_k - \delta_{cR})] \quad (14)$$

$$Q_k = -V_k^2 B_{kk} + V_k V_m [G_{km}\sin(\theta_k - \theta_m) - B_{km}\cos(\theta_k - \theta_m)] + V_k V_{cR}[G_{km}\sin(\theta_k - \delta_{cR}) - B_{km}\cos(\theta_k - \delta_{cR})] \quad (15)$$

And for series converter are:

$$P_{cR} = V_{cR}^2 G_{mm} + V_{cR} V_k [G_{km}\cos(\delta_{cR} - \theta_k) + B_{km}\sin(\delta_{cR} - \theta_k)] + V_m V_{cR}[G_{mm}\cos(\delta_{cR} - \theta_m) + B_{mm}\sin(\delta_{cR} - \theta_m)] \quad (16)$$

$$Q_{cR} = -V_{cR}^2 B_{mm} + V_{cR} V_k [G_{km}\sin(\delta_{cR} - \theta_k) - B_{km}\cos(\delta_{cR} - \theta_k)] + V_m V_{cR}[G_{mm}\sin(\delta_{cR} - \theta_m) - B_{mm}\cos(\delta_{cR} - \theta_m)] \quad (17)$$

The system of equations for SSSC is as follows:

$$\begin{bmatrix} \Delta P_k \\ \Delta P_m \\ \Delta Q_k \\ \Delta Q_m \\ \Delta P_{mk} \\ \Delta Q_{mk} \end{bmatrix} = \begin{bmatrix} \frac{\partial P_k}{\partial \theta_k} & \frac{\partial P_k}{\partial \theta_m} & V_k\frac{\partial P_k}{\partial V_k} & V_m\frac{\partial P_k}{\partial V_m} & \frac{\partial P_k}{\partial \delta_{cR}} & V_{cR}\frac{\partial P_k}{\partial V_{cR}} \\ \frac{\partial P_m}{\partial \theta_k} & \frac{\partial P_m}{\partial \theta_m} & V_k\frac{\partial P_m}{\partial V_k} & V_m\frac{\partial P_m}{\partial V_m} & \frac{\partial P_m}{\partial \delta_{cR}} & V_{cR}\frac{\partial P_m}{\partial V_{cR}} \\ \frac{\partial Q_k}{\partial \theta_k} & \frac{\partial Q_k}{\partial \theta_m} & V_k\frac{\partial Q_k}{\partial V_k} & V_m\frac{\partial Q_k}{\partial V_m} & \frac{\partial Q_k}{\partial \delta_{cR}} & V_{cR}\frac{\partial Q_k}{\partial V_{cR}} \\ \frac{\partial Q_m}{\partial \theta_k} & \frac{\partial Q_m}{\partial \theta_m} & V_k\frac{\partial Q_m}{\partial V_k} & V_m\frac{\partial Q_m}{\partial V_m} & \frac{\partial Q_m}{\partial \delta_{cR}} & V_{cR}\frac{\partial Q_m}{\partial V_{cR}} \\ \frac{\partial P_{mk}}{\partial \theta_k} & \frac{\partial P_{mk}}{\partial \theta_m} & V_k\frac{\partial P_{mk}}{\partial V_k} & V_m\frac{\partial P_{mk}}{\partial V_m} & \frac{\partial P_{mk}}{\partial \delta_{cR}} & V_{cR}\frac{\partial P_{mk}}{\partial V_{cR}} \\ \frac{\partial Q_{mk}}{\partial \theta_k} & \frac{\partial Q_{mk}}{\partial \theta_m} & V_k\frac{\partial Q_{mk}}{\partial V_k} & V_m\frac{\partial Q_{mk}}{\partial V_m} & \frac{\partial Q_{mk}}{\partial \delta_{cR}} & V_{cR}\frac{\partial Q_{mk}}{\partial V_{cR}} \end{bmatrix} \quad (18)$$

7. MODELING OF POWER SYSTEMS WITH UPFC

For the purpose of fundamental frequency steady-state analysis an equivalent circuit consisting of two coordinated synchronous voltage sources should represent the UPFC adequately. Such an equivalent circuit is shown in Figure 3. The synchronous voltage sources represent the fundamental Fourier series component of the switched voltage waveforms at the AC converter terminals of the UPFC [7].

The UPFC voltage sources are:

$$E_{vR} = V_{vR}(\cos\delta_{vR} + J\sin\delta_{vR}) \quad (19)$$

$$E_{cR} = V_{cR}(\cos\delta_{cR} + J\sin\delta_{cR}) \quad (20)$$

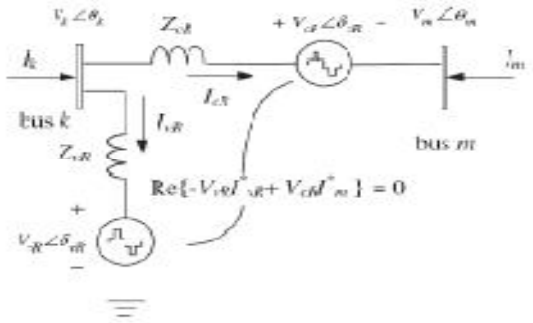

Figure 3: UPFC Equivalent Circuit.

Where V_{vR} and δ_{vR} are the controllable magnitude $V_{vRmin} \le V_{vR} \le V_{vRmax}$ and phase angle $(0 \le \delta_{vR} \le 2\pi)$ of the voltage source representing the shunt converter. The magnitude V_{cR} and phase angle δ_{cR} of the voltage source representing the series converter are controlled between limits $V_{cRmin} \le V_{cR} \le V_{cRmax}$ and $(0 \le \delta_{cR} \le 2\pi)$ respectively. The phase angle of the series-injected voltage determines the mode of power flow control. If δ_{cR} in phase with the nodal voltage angle θ_k, the UPFC regulates the terminal voltage. If δ_{cR} is in quadrature with respect to θ_k it controls active power flow, acting as a phase shifter. If δ_{cR} is in quadrature with the line current angle then it controls active power flow, acting as a variable series compensator [3]. At any other value of δ_{cR}, the UPFC operates as a combination of voltage regulator, variable series compensator, and phase shifter. The magnitude of the series-injected voltage determines the amount of power flow to be controlled.

Based on the equivalent circuit shown in Figure 3 and Equations (17) and (18), the active and reactive

power equations are at bus k [4]:

$$P_k = V_k^2 G_{kk} + V_k V_m [G_{km}\cos(\theta_k - \theta_m) + B_{km}\sin(\theta_k - \theta_m)] V_k V_{cR} [G_{km}\cos(\theta_k - \delta_{cR}) + B_{km}\sin(\theta_k - \delta_{cR})] + V_k V_{vR} [G_{vR}\cos(\theta_k - \delta_{vR}) + B_{vR}\sin(\theta_k - \delta_{vR})] \quad (21)$$

$$Q_k = -V_k^2 B_{kk} + V_k V_m [G_{km}\sin(\theta_k - \theta_m) - B_{km}\cos(\theta_k - \theta_m)] + V_k V_{cR} [G_{km}\sin(\theta_k - \delta_{cR}) - B_{km}\cos(\theta_k - \delta_{cR})] + V_{vR} V_k [G_{vR}\sin(\theta_k - \delta_{vR}) - B_{vR}\cos(\theta_k - \delta_{vR})] \quad (22)$$

At bus m:

$$P_m = V_m^2 G_{mm} + V_m V_k [G_{mk}\cos(\theta_m - \theta_k) + B_{mk}\sin(\theta_m - \theta_k)] + V_m V_{cR} [G_{mm}\cos(\theta_m - \delta_{cR}) + B_{mm}\sin(\theta_m - \delta_{cR})] \quad (23)$$

$$Q_m = -V_m^2 B_{mm} + V_m V_k [G_{mk}\sin(\theta_m - \theta_k) - B_{mk}\cos(\theta_m - \theta_k)] + V_m V_{cR} [G_{mm}\sin(\theta_m - \delta_{cR}) - B_{mm}\cos(\theta_m - \delta_{cR})] \quad (24)$$

Series converter:

$$P_{cR} = V_{cR}^2 G_{mm} + V_{cR} V_k [G_{km}\cos(\delta_{cR} - \theta_k) + B_{km}\sin(\delta_{cR} - \theta_k)] + V_m V_{cR} [G_{mm}\cos(\delta_{cR} - \theta_m) + B_{mm}\sin(\delta_{cR} - \theta_m)] \quad (25)$$

$$Q_{cR} = -V_{cR}^2 B_{mm} + V_{cR} V_k [G_{km}\sin(\delta_{cR} - \theta_k) - B_{km}\cos(\delta_{cR} - \theta_k)] V_{cR} [G_{mm}\sin(\delta_{cR} - \theta_m) - B_{mm}\cos(\delta_{cR} - \theta_m)] \quad (26)$$

Shunt converter:

$$P_{vR} = -V_{vR}^2 G_{vR} + V_{vR} V_k [G_{vR}\cos(\delta_{vR} - \theta_k) + B_{vR}\sin(\delta_{vR} - \theta_k)] \quad (27)$$

$$Q_{vR} = V_{vR}^2 B_{vR} + V_{vR} V_k [G_{vR}\sin(\delta_{vR} - \theta_k) - \cos(\delta_{vR} - \theta_k)] \quad (28)$$

The UPFC power equations, in linearized form, are combined with those of the AC network. For the case when the UPFC controls the following parameters:
1 Voltage magnitude at the shunt converter terminal,2 Active power flow from bus m to bus k,
3 Reactive power injected at bus m, and taking bus m to be a PQ bus.
The linearized system of equation is as follows [4]:

$$\begin{bmatrix} \Delta P_k \\ \Delta P_m \\ \Delta Q_k \\ \Delta Q_m \\ \Delta P_{mk} \\ \Delta Q_{mk} \\ \Delta P_{bb} \end{bmatrix} = \begin{bmatrix} \frac{\partial P_k}{\partial \theta_k} & \frac{\partial P_k}{\partial \theta_m} & V_{vR}\frac{\partial P_k}{\partial V_{vR}} & V_m\frac{\partial P_k}{\partial V_m} & \frac{\partial P_k}{\partial \delta_{cR}} & V_{cR}\frac{\partial P_k}{\partial V_{cR}} & \frac{\partial P_k}{\partial \delta_{vR}} \\ \frac{\partial P_m}{\partial \theta_k} & \frac{\partial P_m}{\partial \theta_m} & 0 & V_m\frac{\partial P_m}{\partial V_m} & \frac{\partial P_m}{\partial \delta_{cR}} & V_{cR}\frac{\partial P_m}{\partial V_{cR}} & 0 \\ \frac{\partial Q_k}{\partial \theta_k} & \frac{\partial Q_k}{\partial \theta_m} & V_{vR}\frac{\partial Q_k}{\partial V_{vR}} & V_m\frac{\partial Q_k}{\partial V_m} & \frac{\partial Q_k}{\partial \delta_{cR}} & V_{cR}\frac{\partial Q_k}{\partial V_{cR}} & \frac{\partial Q_k}{\partial \delta_{vR}} \\ \frac{\partial Q_m}{\partial \theta_k} & \frac{\partial Q_m}{\partial \theta_m} & 0 & V_m\frac{\partial Q_m}{\partial V_m} & \frac{\partial Q_m}{\partial \delta_{cR}} & V_{cR}\frac{\partial Q_m}{\partial V_{cR}} & 0 \\ \frac{\partial P_{mk}}{\partial \theta_k} & \frac{\partial P_{mk}}{\partial \theta_m} & 0 & V_m\frac{\partial P_{mk}}{\partial V_m} & \frac{\partial P_{mk}}{\partial \delta_{cR}} & V_{cR}\frac{\partial P_{mk}}{\partial V_{cR}} & 0 \\ \frac{\partial Q_{mk}}{\partial \theta_k} & \frac{\partial Q_{mk}}{\partial \theta_m} & 0 & V_m\frac{\partial Q_{mk}}{\partial V_m} & \frac{\partial Q_{mk}}{\partial \delta_{cR}} & V_{cR}\frac{\partial Q_{mk}}{\partial V_{cR}} & 0 \\ \frac{\partial P_{bb}}{\partial \theta_k} & \frac{\partial P_{bb}}{\partial \theta_m} & V_{vR}\frac{\partial P_{bb}}{\partial V_{vR}} & V_m\frac{\partial P_{bb}}{\partial V_m} & \frac{\partial P_{bb}}{\partial \delta_{cR}} & V_{cR}\frac{\partial P_{bb}}{\partial V_{cR}} & \frac{\partial P_{bb}}{\partial \delta_{vR}} \end{bmatrix} \begin{bmatrix} \Delta\theta_k \\ \Delta\theta_m \\ \frac{\Delta V_{vR}}{V_{vR}} \\ \frac{\Delta V_m}{V_m} \\ \Delta\delta_{cR} \\ \frac{\Delta V_{cR}}{V_{cR}} \\ \Delta\delta_{vR} \end{bmatrix} \quad (29)$$

8. TEST CASE AND SIMULATION

Standard 14-bus test network is tested with STATCOM, SSSC and UPFC separately, to investigate the behavior of the two devices in the network.

Power flow program is executed for the base case, without inserting any FACTS-devices.From the calculation of VCPI indexwe can understand the voltage collapse prediction at the buses wherever the voltage is violating the limits or nearer the limits.

Table 1:Voltage collapse prediction index

Bus no	VCPI
1	0.1760
2	0.0679
3	0.2060
4	0.1529
5	0.1300
6	0.2591
7	0.2319
8	0.2184
9	0.2874
10	0.2967
11	0.2827
12	0.2920
13	0.2993
14	0.3408

The VCPI index value is calculated at each bus and the results are tabulated in table one.From table one the best location to position STATCOM is given as bus fourteen.Based on the line stability index FVSI of lines, voltage collapse can be accurately predicted.

the index should be less than 1. The line that gives index value closest to 1 will be the most critical line of the bus and may lead to the whole system instability. The FVSI index value is calculated at each line and the results are tabulated in table two. From table two the best location of SSSC and UPFC is given as the line connecting buses 5 and 6.

Power flow program is executed for 4 cases. The first case is the base case, without inserting any FACTS-devices. Other Cases are the same network with the addition of STATCOM, SSSC and UPFC, respectively. The results of power flow without using any FACTS are outlined in Table 3.

Table 2: Fast voltage stability index (FVSI)

From bus	To bus	FVSI
1	2	0.0250
2	3	0.1075
2	4	0.0019
1	5	0.0820
2	5	0.0262
3	4	0.1577
4	5	0.0038
5	6	0.2318
4	7	0.0974
7	8	0.1616
4	9	0.0185
7	9	0.0857
9	10	0.0013
6	11	0.1030
6	12	0.0490
6	13	0.0794
9	14	0.0112
10	11	0.0826
12	13	0.0328
13	14	0.1078

The 14-bus network is modified to include one STATCOM connected at bus 14, to maintain the nodal voltage magnitude at 1.00p.u. The power flow solution is shown in Tables 3a and 3b whereas thenodal voltage magnitudes and phase angles are given. Convergence is achieved in four iterations to a power mismatch tolerance of 10^{-4}.

The power flow result indicates that the STATCOM generates 0.2383 MVAR in order to keep the voltage magnitude at 1.00 p.u. at bus 14. Use of the STATCOM results in an improved network voltage profile. The slack generator increases its reactive power absorption by almost 2.6% compared with the base case, and the direction of reactive power from bus 14 to bus 13 has been changed. The largest reactive power flow takes place in the transmission line connecting bus 7 and bus 8, which is 0.23046 p.u.

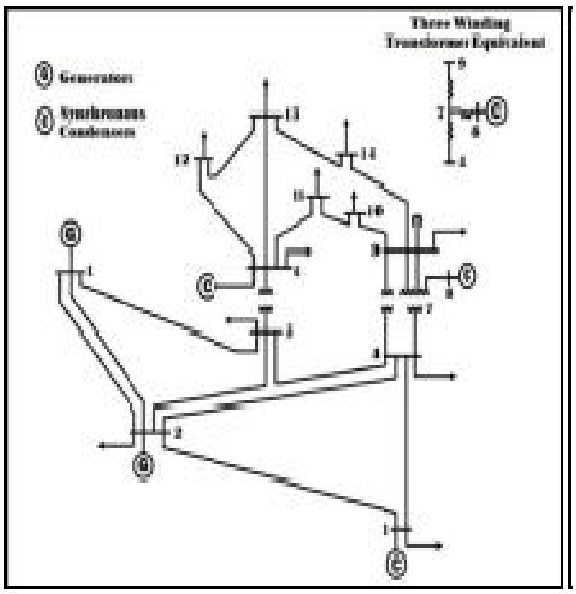

Figure 4: Standard 14-bus Network.

The result value of the STATCOM voltage source is taken to be 1.04 p.u. In general, more reactive power is available in the network than in the base case, and the generator connected at bus 1 increases its share of reactive power absorption compared with the base case.

Table 3a: Power flow without FACTS: Bus Results

Bus no	Voltage magnitude (p.u).	Angle (rad)
1	1.0600	0.0000
2	1.0450	-0.0231
3	1.0000	-0.2324
4	0.9814	-0.1729
5	0.9893	-0.1431
6	1.0300	-0.2895
7	1.0011	-0.2538
8	1.0400	-0.2538
9	0.9782	-0.2975
10	0.9762	-0.3037
11	0.9975	-0.2997
12	1.0057	-0.3120
13	0.9963	-0.3129
14	0.9587	-0.3323

Table 3b: Power flow without FACTS: Line Results.

From bus	To bus	Power flow	
		P , MW	Q , MVAR
1	2	47.085	11.948
2	3	111.752	8.748
2	4	91.444	14.093
1	5	72.133	20.952
2	5	75.483	13.056
3	4	-25.535	21.918
4	5	-67.300	3.945
5	6	63.272	-12.519
4	7	38.840	-7.882
7	8	0.000	-22.127
4	9	22.135	1.963
7	9	38.840	21.689
9	10	6.979	-0.289
6	11	10.853	11.655
6	12	11.257	4.482
6	13	25.483	13.888
9	14	12.696	1.269
10	11	-5.637	-8.452
12	13	2.546	1.888
13	14	8.582	6.602

Table 4a: Power flow with STATCOM: Bus Results.

Bus no	Voltage magnitude (p.u).	Angle (rad)
1	1.0600	0.0000
2	1.0450	-0.0228
3	1.0100	-0.2323
4	0.9906	-0.1737
5	0.9973	-0.1440
6	1.0500	-0.2858
7	1.0202	-0.2525
8	1.0600	-0.2525
9	1.0017	-0.2944
10	0.9993	-0.3002
11	1.0193	-0.2960
12	1.0286	-0.3079
13	1.0215	-0.3103
14	1.0000	-0.3353

Table 4b: Power flow with STATCOM: Line Results.

From bus	To bus	Power flow	
		P , MW	Q ,MVAR
1	2	46.596	12.096
2	3	111.766	3.610
2	4	91.190	8.842
1	5	72.186	17.229
2	5	75.239	8.437
3	4	-25.494	22.430
4	5	-67.522	6.818
5	6	62.998	-17.912
4	7	38.904	-12.791
7	8	0.000	-23.046
4	9	22.170	-0.699
7	9	38.904	17.956
9	10	6.989	0.207
6	11	10.812	11.090
6	12	11.069	3.565
6	13	25.437	10.273
9	14	12.786	-5.061
10	11	-5.627	-7.954
12	13	2.379	1.012
13	14	8.450	2.263

Table 5a: Power flow with SSSC: Bus Results.

Bus no	Voltage magnitude (p.u).	Angle (rad)
1	1.0600	0.0000
2	1.0450	-0.0227
3	1.0100	-0.2319
4	0.9922	-0.1737
5	0.9922	-0.1444
6	1.0500	-0.2864
7	1.0236	-0.2512
8	1.0600	-0.2512
9	1.0018	-0.2925
10	1.0012	-0.2986
11	1.0251	-0.2954
12	1.0358	-0.3076
13	1.0262	-0.3082
14	0.9858	-0.3260

Table 5b: Power flow with SSSC: Line Results

From bus	To bus	Power flow	
		P , MW	Q , MVAR
1	2	46.404	12.154
2	3	111.592	3.614
2	4	91.085	7.966
1	5	72.300	16.339
2	5	75.331	7.316
3	4	-25.652	21.555
4	5	-66.990	5.820
5	6	65.000	-17.131
4	7	38.459	-13.719
7	8	0.000	-21.178
4	9	21.858	-0.459
7	9	38.459	21.076
9	10	6.635	-1.771
6	11	9.086	8.818
6	12	9.634	1.281
6	13	22.197	8.111
9	14	12.382	0.284
10	11	-5.980	-9.931
12	13	2.639	2.078
13	14	8.894	7.580

The original 14-bus network is modified to include one SSSC to compensate the transmission line connected between bus 5 and bus 6. The SSSC is used to increase active power flowing from bus 5 towards bus 6by 50% line compensation. Convergence is obtained in 4 iterations to a power mismatch tolerance of 10^{-4} . The power flow results are shown in Tables 3a and 3b.

Table 6a: Power flow with UPFC: Bus Results.

Bus no	Voltage magnitude (p.u).	Angle (rad)
1	1.0600	0.0000
2	1.0450	-0.0227
3	1.0100	-0.2320
4	0.9998	-0.1738
5	1.0000	-0.1445
6	1.0500	-0.2863
7	1.0236	-0.2513
8	1.0600	-0.2513
9	1.0017	-0.2925
10	1.0011	-0.2986
11	1.0251	-0.2953
12	1.0358	-0.3075
13	1.0262	-0.3082
14	0.9858	-0.3260

As expected, nodal voltage magnitudes do not change considerably compared with the base case. The result value of the SSSC voltage source is taken to be V_{cR} =0.020p.u.

The 14-bus network is modified to include one UPFC to compensate the transmission line linking bus 5and bus 6. The UPFC is caused to maintain active and reactive powers leaving the UPFC, towards bus 14, at 0.65p.u. and -0.16804p.u, respectively. Moreover, the UPFC shunt converter is set to regulate the nodal voltage magnitude at bus 5 at 1.00p.u. The result values of the UPFC voltage sources are taken to be V_{cR} =0.02 p.u, V_{vR} =1.02 p.u. Convergence is obtained in four iterations to a power mismatch tolerance of10^{-4} . The power flow results are shown in Tables 4 a and b. The real and reactive power losses in four cases are tabulated in table seven.

Table 6b: Power flow with UPFC: Line Results.

From bus	To bus	Power flow	
		P , MW	Q ,WVAR
1	2	46.517	12.119
2	3	111.619	3.614
2	4	90.394	3.744
1	5	72.317	15.952
2	5	75.266	6.846
3	4	-27.405	17.762
4	5	-62.906	20.483
5	6	65.000	-16.804
4	7	38.731	-10.080
7	8	0.000	-21.213
4	9	22.013	0.959
7	9	38.431	21.080
9	10	6.609	-1.774
6	11	9.113	8.822
6	12	9.638	1.281
6	13	22.211	8.114
9	14	12.365	0.282
10	11	-6.006	-9.933
12	13	2.643	2.078
13	14	8.911	7.582

Table 7: Real and Reactive Power losses

Type of loss	Without FACTS	With STATCOM	With SSSC	With UPFC
1.Real power loss MW	18.999	18.550	18.322	18.153
2.Reactive power loss MVAR	84.434	83.126	82.441	81.654

9. CONCLUSION

This paper presented the modeling and simulation methods required for study of the steady-state operation of electrical power systems with FACTS controllers: STATCOM, SSSC, and UPFC. The VCPI and NLSI are calculated for locating the FACTS devices. The conventional power flow solution could systematically be modified to include multiple FACTS controllers: STATCOM, SSSC, and UPFC. It was shown that the effect of FACTS controllers on power flow can be provided by adding new entries and adjusting some existing entries in the linearized Jacobean equation of the basic system with no FACTS controllers.

An existing power flow program that uses the Newton–Raphson method of solution in Cartesian coordinates can easily be modified through the procedure presented in this paper. This procedure was applied on the 14-bus power system and implemented using the MATLAB® software package. The numerical results show the robust convergence of the presented procedure. The steady state models of STATCOM, SSSC, and UPFC are evaluated in Newton-Raphson algorithm and the results show that UPFC can mostly carry out the aim of both SSSC and STATCOM.

REFERENCES

[1] Povh, D. 2000. **Modeling of FACTS in Power System Studies.***Proc. IEEE Power Eng. Soc. Winter Meeting. 2:1435–1439.*

[2] Zhang, X.P. 2003. **Advanced Modeling of Multicontrol Functional Static Synchronous Series Compensator (SSSC) in Newton–Raphson Power Flow.***IEEE Trans. Power Syst. 18(4):1410–1416*

[3] Zhang, X.P., C.F. Xue, and K.R. Godfrey. 2004. **Modelling of the Static Synchronous Series Compensator (SSSC) n Three-Phase Newton Power Flow.***IEEE Proc.-Gener. Transm. Distrib. 151(4).*

[4] P.Kessal H.Glavitsch **Estimating the voltage stability of a power system** *IEEE .Transaction on Power Delivary .vol.PWRD-1.N3.july 1986.*

[5] Acha, E., C.R. Fuerte-Esquivel, H. Ambriz-Pe´rez, and C. Angeles-Camacho. 2004**.** ***FACTS: Modelling and Simulation in Power Networks.*** John Wiley and Sons: West Sussex, UK.

[6] Radman, G. and R.S. Raje. 2007. ***Power Flow Model/Calculation for Power Systems with Multiple FACTS Controllers.*** *Electric Power Systems Research*. 77:1521–1531.

[7] Stagg, G.W. and A.H. Ei-Abiad. 1968. ***Computer Methods in Power Systems Analysis.*** McGraw-Hill: New York, NY.

[8] Hingorani, N.G. and L. Gyugyi. 2000. ***Understanding FACTS: Concepts and Technology of Flexible AC Transmission Systems.*** Wiley–IEEE Press: New York, NY. ISBN: 0-7803-3464-7.

[9] Zhang, X.P., C. Rehtanz, and B. Pal. 2006. ***Flexible AC Transmission Systems: Modelling and Control.*** Springer Verlag: Berlin, Germany.

[10] Sahoo, A.K., S.S. Dash, and T. Thyagarajan. 2007. ***Modeling of STATCOM and UPFC for Power System Steady State Operation and Control.*** IET-UK International Conference on Information and Communication Technology in Electrical Sciences (ICTES 2007).

[11] Tong Zhu, GarngHuang, ***Find the accurate point of voltage collapse in real-time.****in* Proc. of the 21st IEEE International Conference on Power Industry Computer Applications, PICA '99,Santa Clara, CA, May 1999